Environmental Science & Technology

Article

pubs.acs.org/est

Sunlight Inactivation of Viruses in Open-Water Unit Process Treatment Wetlands: Modeling Endogenous and Exogenous Inactivation Rates

Andrea I. Silverman,[†,‡] Mi T. Nguyen,[†,‡] Iris E. Schilling,[‡,§] Jannis Wenk,[†,‡,∥] and Kara L. Nelson*[,†,‡]

[†]Department of Civil & Environmental Engineering, University of California, Berkeley, California 94720-1710, United States

[‡]Engineering Research Center for Re-Inventing the Nation's Urban Water Infrastructure (ReNUWIt), Berkeley, California 94305, United States

[§]Institute of Biogeochemistry and Pollutant Dynamics, ETH Zurich, CH-8092 Zurich, Switzerland

Supporting Information

ABSTRACT: Sunlight inactivation is an important mode of disinfection for viruses in surface waters. In constructed wetlands, for example, open-water cells can be used to promote sunlight disinfection and remove pathogenic viruses from wastewater. To aid in the design of these systems, we developed predictive models of virus attenuation that account for endogenous and exogenous sunlight-mediated inactivation mechanisms. Inactivation rate models were developed for two viruses, MS2 and poliovirus type 3; laboratory- and field-scale experiments were conducted to evaluate the models' ability to estimate inactivation rates in a pilot-scale, open-water, unit-process wetland cell. Endogenous inactivation rates were modeled using either photoaction spectra or total, incident UVB irradiance. Exogenous inactivation rates were modeled on the basis of virus susceptibilities to singlet oxygen. Results from both laboratory- and field-scale experiments showed good agreement between measured and modeled inactivation rates. The modeling approach presented here can be applied to any sunlit surface water and utilizes easily measured inputs such as depth, solar irradiance, water matrix absorbance, singlet oxygen concentration, and the virus-specific apparent second-order rate constant with singlet oxygen (k_2). Interestingly, the MS2 k_2 in the open-water wetland was found to be significantly larger than k_2 observed in other waters in previous studies. Examples of how the model can be used to design and optimize natural treatment systems for virus inactivation are provided.

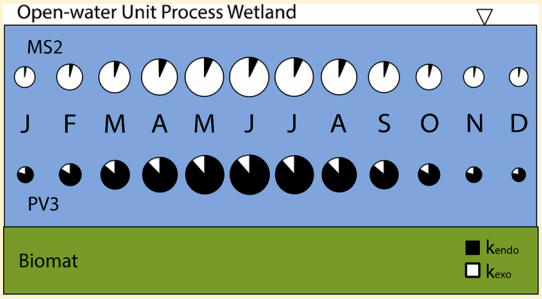

INTRODUCTION

Natural wastewater treatment systems, including constructed wetlands, have a demonstrated ability to reduce waterborne virus concentrations,[1−3] with sunlight playing an important role in virus inactivation.[4,5] While significant research has been devoted to determining waterborne virus susceptibilities to sunlight inactivation,[6−13] little has been done to integrate these data into mechanistic models of virus inactivation in sunlit waters.[14] The goal of this research was to develop sunlight inactivation models and evaluate their ability to predict virus inactivation rates in a pilot-scale, open-water cell in a unit-process treatment wetland. Such models can be used to optimize treatment system design for virus removal and predict whether disinfection goals are met. Given that viruses can be more resistant than traditional bacterial indicator organisms to engineered[15−17] and natural[18,19] treatment processes, it is important to develop quantitative models to describe key virus removal mechanisms.

Unit-process wetlands contain individual cells designed to optimize specific contaminant-removal processes; wetland cells can be incorporated with mechanical treatment systems or placed in series to form a treatment train of their own.[3] Regarding the role of sunlight in virus removal,[4,5,20] open-water cells provide an opportunity to enhance inactivation by allowing more sunlight exposure than vegetated cells.[3] While the focus of this study is on open-water wetland cells, the modeling approach can be applied to other sunlit waters, including waste stabilization ponds, recreational waters, and SODIS vessels.

There are three proposed sunlight inactivation mechanisms for viruses:[4,6] the direct- and indirect-endogenous mechanisms require absorption of photons by virus components, while the exogenous mechanism is initiated by light absorption by external photosensitizers [e.g., natural organic matter (NOM)]. After photon absorption, excited states of photosensitizers may react directly with viruses[9] or produce reactive species that can cause inactivating damage. The direct- and indirect-endogenous mechanisms are difficult to separate experimentally, and both rely on photon absorption by viruses; they are therefore

Received: October 11, 2014
Revised: January 16, 2015
Accepted: January 21, 2015

DOI: 10.1021/es5049754
Environ. Sci. Technol. XXXX, XXX, XXX−XXX

referred to jointly as the "endogenous mechanism" (see Silverman et al.[6]).

The modeling approach presented here expands upon past research on virus inactivation rate models. Previously, Fisher et al.[21] developed photoaction spectra (PAS) for the endogenous inactivation of MS2 and PRD1 coliphages in waters that did not contain light-attenuating or photosensitizing molecules; Nguyen et al.[22] validated that the PAS inactivation rate model was able to predict endogenous MS2 inactivation rates with exposure to natural sunlight and in the presence of light-attenuating compounds. Mattle et al.[14] developed a model that includes both endogenous and exogenous inactivation. Endogenous inactivation was modeled using a virus inactivation quantum yield; to model exogenous inactivation, second-order rate constants were determined for four reactive species: singlet oxygen ($^1O_2$), hydroxyl radicals ($OH^\bullet$), triplet-state organic matter (^3OM), and carbonate radicals. However, only $^1O_2$ was found to contribute significantly to exogenous inactivation, which is consistent with previous research that found exogenous inactivation rates to scale with $^1O_2$ concentration.[6,9,11] In the present study, we build upon this prior work by developing an inactivation rate model that includes both endogenous and exogenous mechanisms, and evaluating its ability to predict inactivation rates in a pilot-scale open-water wetland. Given the dual effect of light-attenuating photosensitizers on inactivation rates (i.e., decreasing endogenous inactivation and contributing to exogenous inactivation), our inactivation rate model includes both mechanisms and accounts for the effect of environmental conditions (e.g., sunlight irradiance, light attenuation, water quality, reactive species concentrations, depth, and mixing) on observed inactivation rates.

Susceptibility to endogenous and exogenous inactivation differs among virus species and types,[6−8,10,14,23] necessitating the development of virus-specific values for key parameters in model equations. MS2 and human poliovirus type 3 (PV3), both single-stranded RNA viruses, were chosen as model viruses for this research based on their different susceptibilities to inactivation: PV3 has a faster endogenous inactivation rate than MS2, while MS2 is more susceptible to the exogenous mechanism.[6,10] The research presented below was organized into three tasks: (1) virus-specific parameters in model equations were determined using data from previous studies and new experiments; (2) laboratory experiments were conducted to determine if model equations could approximate MS2 and PV3 inactivation rates in small batches of wetland water at two water column depths under simulated sunlight; (3) bacteriophage inactivation was monitored in a pilot-scale open-water wetland cell, and measured F+RNA coliphage inactivation rates were compared to modeled values for MS2, which is a member of the F+RNA coliphage family. MS2 was previously found to have endogenous[10] and exogenous[23] inactivation rates that were similar to those of other F+RNA coliphages.

METHODS

Discovery Bay Wastewater Treatment Wetland. The Discovery Bay constructed wetland (Figure S4, Supporting Information) is a pilot-scale system located in Discovery Bay, CA (37°54′ N, 121°36′ W).[24,25] The wetland consists of unit-process cells that receive nitrified, nondisinfected effluent from an adjacent oxidation ditch wastewater treatment facility. The unit-process cells include an open-water, nonvegetated cell that was designed to promote photolysis: it is shallow (approximately 20 cm deep) to allow sunlight penetration and lined with a geotextile fabric and concrete to prevent the growth of emergent vegetation, which would block sunlight. On the bottom of the wetland, a 2−7 cm thick biomat layer containing a community of photosynthetic, and other associated, microorganisms has naturally accumulated. During the study, the open-water cell had a surface area of 400 m^2 and received approximately 23 000 gal (86 m^3) of wastewater per day, resulting in a flow rate of approximately 1 L/s and a theoretical hydraulic residence time (HRT) of 0.93 d. The average surface biochemical oxygen demand (BOD) loading rate was 6.45 kg ha^{-1} d^{-1}. The cell contained baffles to promote plug flow hydraulics.

Wetland water used in laboratory experiments was collected from the outlet of the open-water cell (pH 8.5−9.0). After collection, water was filtered using 5 μm pore size, polycarbonate membrane filters (Nucleopore), stored at 4 °C in the dark and used within one month. UV−vis absorbance spectra of filtered and unfiltered water were measured with a spectrophotometer (Shimadzu UV-2600; l = 1 cm; Figure S5, Supporting Information); Mg^{2+} concentrations were measured by ICP-MS (Agilent Technologies 7700 series). The absorbance spectra and dissolved organic carbon concentrations in the open-water cell were not found to change significantly between the inlet and outlet or over time.[26]

Sunlight Inactivation Model Equations. In this paper we use k_{obs} terms to denote experimentally *measured* inactivation rates, while k_{endo} and k_{exo} are used to denote *modeled* endogenous and exogenous inactivation rates, respectively. k_{tot} terms are total *modeled* inactivation rates, which are calculated as the sum of k_{endo} and k_{exo}; while there could be interaction between mechanisms, there is currently no evidence of this. The superscript "L" is used to denote measured and modeled inactivation rates in the laboratory, and "W" is used to denote those in the wetland.

$$k_{tot}^{L} = k_{endo}^{L} + k_{exo}^{L} \quad (1)$$

$$k_{tot}^{W} = k_{endo}^{W} + k_{exo}^{W} \quad (2)$$

Given that average dark inactivation rates (k_{dark}) measured in this study and others[6,10,11,14] were much smaller than those observed with sunlight exposure (Table S3, Supporting Information), we did not include k_{dark} in the model. If k_{dark} were significant under other conditions, the model would underestimate the value of k_{tot}.

To use the equations presented below to predict k_{endo} and k_{exo}, the required inputs are water column depth (z, cm), wavelength-specific decadic absorbance [$\alpha(\lambda)$, cm^{-1}], wavelength-specific irradiance incident on the water surface [$E_d(0,\lambda)$, W m^{-2}], the solar zenith angle (γ), the bulk-phase, steady-state singlet oxygen concentration ($[^1O_2]_{ss,bulk}$, M), the dissolved organic carbon concentration ([DOC], mg/L), and the apparent second-order reaction rate constant between each virus and $^1O_2$ (k_2, M^{-1} h^{-1}). While the former inputs are easy to measure or predict, k_2 must be measured in laboratory experiments for specific water−virus combinations. A summary of the modeling equations and terms is provided in the Supporting Information.

Modeling Light Attenuation. Both endogenous and exogenous inactivation mechanisms depend on light transmitted through the water column. Natural waters alter the light field through absorption and scattering, and measurements of

DOI: 10.1021/es5049754
Environ. Sci. Technol. XXXX, XXX, XXX−XXX

light irradiance incident on the water surface must be corrected for these effects. Average scalar light irradiance over a well-mixed depth [$\langle E_0(z,\lambda)\rangle$, W m^{-2}] was calculated using the following relationship (see the Supporting Information for details):[22,27]

$$\langle E_0(z,\lambda)\rangle = E_d(0,\lambda)\left(\frac{1-e^{-2.303\psi\alpha(\lambda)z}}{2.303\psi\alpha(\lambda)z}\right) \quad (3)$$

Average values of $\alpha(\lambda)$ in 5 μm filtered water were used to model light attenuation during laboratory experiments, and average values of $\alpha(\lambda)$ in unfiltered water were used when modeling the wetland (Figure S5, Supporting Information). ψ is a path length correction factor used to correct z for light-path geometry; ψ was assumed to equal 1 in the laboratory (i.e., the solar simulator used in experiments created a collimated beam of light) and was calculated for the wetland using the following equation:[28]

$$\psi = \left(\sqrt{1-(n^{-1}\sin\gamma)^2}\right)^{-1} \quad (4)$$

where γ is the solar zenith angle and n is the index of refraction (~1.34 for water).[29] Light scattering was found to be negligible[22] and was not accounted for in the model.

$E_d(0,\lambda)$ used for modeling inactivation in the laboratory was measured with a spectroradiometer. $E_d(0,\lambda)$ and γ used for modeling inactivation in the wetland were predicted by the simple model of the atmospheric radiative transfer of sunshine (SMARTS; global horizontal irradiance)[30] for each hour on the 21st day of each month at 40° N (inputs to SMARTS are presented in Table S2, Supporting Information). SMARTS accounts for diurnal and seasonal changes in light intensity. However, SMARTS assumes clear-sky conditions and does not account for variations in atmospheric conditions or cloud cover.

Modeling Inactivation Rates in the Laboratory. On the basis of previous research,[6,10−12,21,22] endogenous inactivation was modeled using two approaches. The first approach to calculating k^L_{endo} (h^{-1}) employs a PAS, which accounts for the sensitivity of the organism to different wavelengths. The PAS for MS2 was determined by Fisher et al.[21] and is used in the following equation:

$$k^L_{endo,PAS} = \sum_\lambda \langle E_0(z,\lambda)\rangle\, P(\lambda)\, \Delta\lambda \quad (5)$$

$P(\lambda)$ (m^2 W^{-1} h^{-1}) is the wavelength- and virus-dependent spectral sensitivity coefficient; $\Delta\lambda$ is equal to 3 nm.[21] $P(\lambda)$ values for MS2 are provided in Table S1 of the Supporting Information; $P(\lambda)$ values for PV3 have not yet been determined.

The second endogenous inactivation modeling approach, referred to here as the total UVB (tUVB) model, recognizes that endogenous inactivation of MS2 and PV3 only occurs with exposure to UVB irradiance (λ = 280−320 nm).[6,10,11] In the tUVB model, all UVB wavelengths are weighted equally, and we define β (m^2 W^{-1} h^{-1}) as the correlation factor between the sum of irradiance in the UVB range and k_{endo}:

$$k^L_{endo,tUVB} = \beta \sum_{320}^{\lambda=280} \langle E_0(z,\lambda)\rangle \quad (6)$$

To determine β for MS2 and PV3, we compiled data on virus inactivation rates in sensitizer-free water from previous publications[6,10,11,21] and new simulated-sunlight inactivation experiments (see the section "Laboratory Experiments"); sensitizer-free water was used to exclude exogenous inactivation. Linear regression analysis between k_{obs} and total UVB irradiance was performed to determine β for each virus.

Under environmental conditions, exogenous sunlight inactivation appears to be important for some viruses (e.g., MS2) but limited for others (e.g., PV3).[6] While additional reactive species are involved in MS2 exogenous inactivation,[9,14] $^1O_2$ was previously found to be the most important,[11,14] and measured exogenous inactivation rates were found to scale with $[^1O_2]_{ss,bulk}$.[6,9,11] Therefore, k^L_{exo} was calculated as a pseudo-first-order rate constant using the following equation:

$$k^L_{exo} = k_2[^1O_2]_{ss,bulk} \quad (7)$$

k_2 is an apparent value that must be determined for specific water−virus combinations. It was measured during solar simulator experiments using a filter that blocks out UVB light; with no incident UVB light, it is assumed that all observed inactivation was caused by the exogenous mechanism.[6,10,11] k_2 was calculated from experimental data by dividing inactivation rates ($k^L_{obs,exo}$) by measured $[^1O_2]_{ss,bulk}$. Due to its short lifetime, $^1O_2$ exists in higher concentrations close to its source of production than in bulk solution.[31] Therefore, k_2 is an apparent value: depending on the proximity of the virus to photosensitizers, the $^1O_2$ concentration viruses are exposed to can differ from measured $[^1O_2]_{ss,bulk}$ used to calculate k_2. k_2 is also affected by the susceptibility of a particular virus to oxidative damage.[6,12,14]

Modeling Inactivation Rates in the Discovery Bay Open-Water Wetland Cell. To model k^W_{tot}, we assumed a 20 cm deep, well-mixed water column throughout the open-water cell. To account for the effect of the biomat on inactivation rates, we followed assumptions made by Jasper et al.:[25] the biomat had an average depth of 5 cm, leaving a light-exposed water column depth (z) of 15 cm. Calculated inactivation rates were multiplied by a shading factor of 0.75 (15 cm/20 cm) to account for the time viruses resided within the biomat. Given diurnal cycles in light intensity, inactivation rates in the wetland were predicted as 24 h average values.

Endogenous inactivation rates (k^W_{endo}, d^{-1}) in the open-water cell were predicted with the PAS and tUVB models in a manner similar to that in the laboratory, but using 24 h average $\langle E_0(z,\lambda)\rangle$ (calculated as the average of hourly values). Equations were multiplied by 24 h/d to convert units to d^{-1}:

$$k^W_{endo,PAS} = 24\sum_\lambda \langle E_0(z,\lambda)\rangle_{24\,h\,avg}\, P(\lambda)\, \Delta\lambda \quad (8)$$

$$k^W_{endo,tUVB} = 24\beta \sum_{320}^{\lambda=280} \langle E_0(z,\lambda)\rangle_{24\,h\,avg} \quad (9)$$

Exogenous inactivation rates in the open-water cell (k^W_{exo}, d^{-1}) were predicted using the following equation:

$$k^W_{exo} = 24k_2[^1O_2]_{ss,bulk,mod} \quad (10)$$

Modeled $^1O_2$ concentrations ($[^1O_2]_{ss,bulk,mod}$; M) were used to predict k^W_{exo}. $[^1O_2]_{ss,bulk,mod}$ values were 24 h average values, calculated following the approach used by Jasper and Sedlak:[24] $[^1O_2]_{ss,bulk,mod}$ was approximated by adjusting near-surface, summer-noon $[^1O_2]_{ss,bulk}$ per milligram of DOC [estimated to be ~1 × 10^{-14} M/(mg of DOC) by Haag and Hoigné][32] for light attenuation at 410 nm, as this wavelength was previously found to best predict $[^1O_2]_{ss,bulk}$.[32]

DOI: 10.1021/es5049754
Environ. Sci. Technol. XXXX, XXX, XXX−XXX

$$[^1O_2]_{ss,bulk,mod} = (1 \times 10^{-14})[DOC]\frac{\langle E_0(z, \lambda = 410)\rangle_{24\,h\,avg}}{\langle E_d(0, \lambda = 410)\rangle_{June\text{-}noon}} \quad (11)$$

An average value of 8 mg/L-C[25] was input for [DOC] in the open-water cell.

Determining Uncertainty in Model Results. Uncertainties in k_{tot}, k_{endo}, and k_{exo} were determined by Gaussian error propagation. Errors on k_2 and β were the standard errors determined from experimental data. Errors on $k_{endo,PAS}$ and $[^1O_2]_{ss,bulk,mod}$ were set at 15% of the calculated values, based on the typical error reported by Nguyen et al.[22] and Haag and Hoigné.[32]

Laboratory Experiments. Comprehensive MS2 (ATCC 15597-B1) and PV3 (ATCC VR-300) propagation, purification, and enumeration methods are provided in the Supporting Information.

Methods for bench-scale inactivation experiments were similar to those of previous research in our laboratory;[6,10−12] details are provided in the Supporting Information. Briefly, experiments were conducted using a 1000 W solar simulator (Oriel) with either an atmospheric attenuation filter to mimic the solar spectrum or a UVB-blocking filter to exclude endogenous inactivation. Bulb irradiance was measured at the start of each experiment using a spectroradiometer (EPP2000C-SR-100 with CR2 cosine receptor, Stellarnet; average irradiance spectra are provided in Figure S6, Supporting Information). Experimental reactors consisted of glass beakers painted black on the outside; reactors were constantly mixed and located in a water bath cooled to 20 °C. During experiments, 0.5 mL subsamples were removed from the reactors every 1−2 h, placed on ice, and analyzed for virus concentrations within 6 h of collection.

Three sets of laboratory experiments were conducted at different times using different water samples. First, to determine β, viruses were inoculated into clear, sensitizer-free solution (PBS: 16 mM Na_2HPO_4, 4 mM NaH_2PO_4, and 10 mM NaCl; 62 mM ionic strength) and exposed to full-spectrum light of various intensities. Second, to determine k_2 values for MS2 and PV3 that were specific to water from the Discovery Bay open-water cell, viruses were inoculated into wetland water and exposed to UVB-blocked, simulated sunlight [average total irradiance (280−700 nm), 235 W m^{-2}; UVB irradiance (280−320 nm), 0.2 W m^{-2}; UVA irradiance (320−400 nm), 21 W m^{-2}]. $[^1O_2]_{ss,bulk}$ was measured in identical reactors, but using furfuryl alcohol as a probe[33] (see the Supporting Information for details). Third, to determine the ability of model equations to approximate measured inactivation rates, k^L_{obs} was measured and compared to the predicted k^L_{tot}. To investigate the effect of light attenuation on inactivation rates, experiments were conducted in reactors with two different water column depths. Viruses were inoculated into 200 mL beakers filled with either 100 mL of PBS or 100 mL of wetland water and 4 L beakers filled with 3.5 L of wetland water, resulting in water column depths of 5 and 20 cm, respectively. Reactors were exposed to full-spectrum light (average total irradiance, 237 W m^{-2}; UVB irradiance, 1.91 W m^{-2}; UVA irradiance, 28 W m^{-2}); dark controls were covered with aluminum foil. $\alpha(\lambda)$, $E_d(0,\lambda)$, and $[^1O_2]_{ss,bulk}$ were measured during the experiments and used as inputs to the model equations.

First-order, observed inactivation rate constants in the laboratory (k^L_{obs}) were calculated as follows:

$$-\left(\ln\frac{C_t}{C_0}\right) = k^L_{obs}t \quad (12)$$

where C_0 is the initial virus concentration and C_t is the concentration at time t. $\ln(C_t/C_0)$ values were calculated for each time point and replicate; these values were pooled and used to calculate k^L_{obs} ± the standard error of the slope by linear regression. Analysis of variance (ANOVA) with Tukey's post-test (Prism v6.0c, GraphPad Software) was used to determine whether k^L_{obs} values were significantly different from each other.

Coliphage Monitoring in the Discovery Bay Treatment Wetland. Samples were collected two or four times monthly between January and August 2013 from five locations within the open-water cell: the inlet, the turns at the ends of baffles 1, 2, and 3, and the outlet (Figure S4, Supporting Information). All samples were analyzed for concentrations of F+RNA coliphages. June to August samples were also analyzed for somatic coliphages (results in the Supporting Information). Samples were collected using sterile, polypropylene bottles, stored on ice during transport, and processed within 6 h of collection. Sampling only occurred if the sky was not overcast for three consecutive days prior to sample collection. Detailed coliphage enumeration methods are provided in the Supporting Information.

To compare observed coliphage inactivation rates in the open-water cell (k^W_{obs}, d) with the predicted k^W_{tot}, coliphage concentrations measured during wetland monitoring were used to calculate k^W_{obs} using the Wehner−Wilhelm equation.[34] The Wehner−Wilhelm equation assumes first-order kinetics and accounts for nonideal hydraulics due to dispersion:

$$\frac{C_x}{C_0} = \frac{4a\,\exp\left(\frac{1}{2d}\right)}{(1+a)^2\exp\left(\frac{a}{2d}\right) - (1-a)^2\exp\left(-\frac{a}{2d}\right)} \quad (13)$$

$a = (1 + 4k^W_{obs}\theta_x d)^{1/2}$, C_x is the coliphage concentration at sampling location x, C_0 is the concentration at the inlet, d is the dispersion number, and θ_x is the mean HRT at sampling location x. d and the total HRT were determined to be 0.08 and 1.12 d, respectively, on the basis of the Rhodamine-WT tracer test conducted by Jasper et al.[25] (the tracer recovery was 77%). The calculations, and a sensitivity analysis to determine the relative importance of d and the total HRT to k^W_{obs}, can be found in the Supporting Information.

Values of C_x/C_0 were calculated for each sampling location and day. Mean θ_x values were determined by assuming that the HRTs at turns 1, 2, and 3 correspond to 1/3, 1/2, and 2/3 of the overall HRT, respectively, on the basis of the surface area between sampling locations. For each month, C_x/C_0 data from different days were pooled and Solver (Microsoft Excel) was used to calculate k^W_{obs} by minimizing the root-mean-square error between the observed C_x/C_0 values and those predicted by the Wehner−Wilhelm equation.

RESULTS AND DISCUSSION

Model Development. To model k_{tot}, we first determined values for β in $k_{endo,tUVB}$ equations and k_2 in k_{exo} equations. β is the slope of the regression line between the sum of irradiance in the UVB range and k_{obs} measured in sensitizer-free water (Figure S8, Supporting Information); β was found to be 0.12 ± 0.02 m^2 W^{-1} h^{-1} (R^2 = 0.89) for MS2 and 0.94 ± 0.08 m^2 W^{-1} h^{-1} (R^2 = 0.97) for PV3. While β values are virus-specific constants that should not vary across water matrixes, some

DOI: 10.1021/es5049754
Environ. Sci. Technol. XXXX, XXX, XXX−XXX

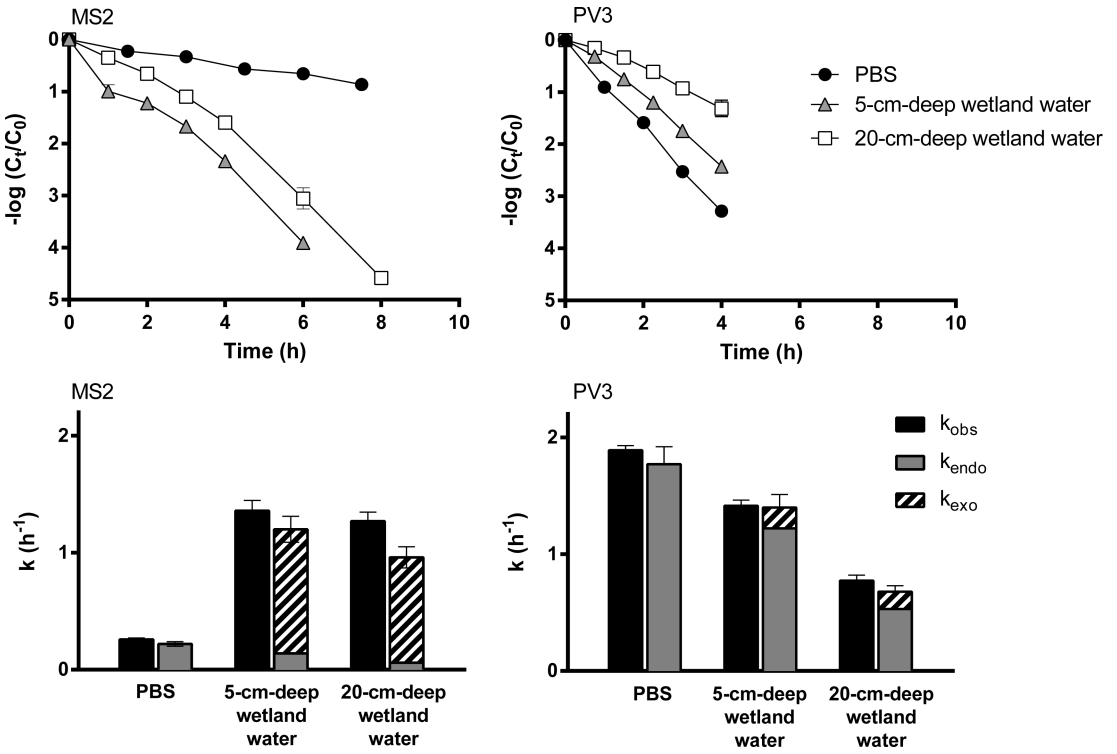

Figure 1. MS2 and PV3 inactivation curves (top row) and inactivation rates (bottom row) during laboratory experiments in clear, sensitizer-free solution (PBS) and 5 and 20 cm deep, 5 μm filtered wetland water (n = 2 for each time point). Measured (k^{L}_{obs}) and modeled (k^{L}_{endo} and k^{L}_{exo}) inactivation rates are presented. k^{L}_{endo} was calculated using the PAS model for MS2 and the total UVB model for PV3. Error bars report the standard error; some error bars are smaller than the symbols.

limitations of the tUVB model exist and are discussed in a subsequent section.

In contrast, k_2 is a value that may vary between waters and must be determined empirically. k_2 values specific to the Discovery Bay open-water cell were found to be $(1.1 \pm 0.04) \times 10^{13}$ M^{-1} h^{-1} for MS2 and $(0.23 \pm 0.03) \times 10^{13}$ M^{-1} h^{-1} for PV3 (Figure S9, Supporting Information).

Measured and Modeled Inactivation Rates in the Laboratory. Experiments were conducted to determine whether model equations could approximate measured virus inactivation rates under controlled conditions (i.e., well-mixed batch reactors and constant light intensity). Measured and modeled inactivation rates in the laboratory are presented in Table S3 (Supporting Information).

MS2 and PV3 inactivation rates were remarkably different from each other and depended on water characteristics (Figure 1). MS2 k^{L}_{obs} was significantly lower in PBS than in wetland water ($p < 0.001$); however, there was no significant difference between MS2 k^{L}_{obs} in 5 and 20 cm deep wetland water columns. In contrast, PV3 k^{L}_{obs} was fastest in PBS ($p < 0.001$) and was significantly slower in 20 cm deep wetland water than in 5 cm deep wetland water ($p < 0.001$). In PBS, PV3 was inactivated at a rate 7 times faster than that of MS2, while in 20 cm deep wetland water MS2 was inactivated almost 2 times faster than PV3. This finding has implications for the use of MS2 as a conservative indicator of sunlight inactivation.

Given that PBS contains no sensitizers, inactivation in PBS is caused by the endogenous mechanism alone. For MS2, the two k^{L}_{endo} models (i.e., the PAS and tUVB models) predicted similar k^{L}_{endo} values in PBS (Figure S10, Supporting Information), and these values were also similar to MS2 k^{L}_{obs} measured in PBS during the experiments. As the PAS has not been determined for PV3, only the tUVB model was used to predict PV3 k^{L}_{endo}. The modeled value of PV3 $k^{L}_{endo,tUVB}$ was also similar to PV3 k^{L}_{obs} measured in PBS.

Model equations were also able to approximate inactivation rates measured in laboratory-scale experiments using wetland water (Figure 1). MS2 k^{L}_{tot} values predicted in 5 and 20 cm deep wetland water were 12% and 25% lower than the measured MS2 k^{L}_{obs}, respectively; PV3 k^{L}_{tot} values predicted in 5 and 20 cm deep wetland water were 2% and 12% lower than PV3 k^{L}_{obs}, respectively. These results indicate that the model was able to capture the dual effects of light-absorbing constituents in wetland water: the decrease in k_{endo} due to light attenuation and the increase in k_{exo} due to photosensitized production of reactive species.

For MS2, k^{L}_{endo} was small in wetland water, and inactivation was dominated by the exogenous mechanism. This finding is consistent with previous research that found MS2 to be quite susceptible to exogenous inactivation.[6,11] The dominance of the exogenous mechanism for MS2 was also confirmed by similar k^{L}_{obs} values in the two well-mixed wetland water depths, despite more light attenuation in the 20 cm deep reactor. This was due to similar $[^1O_2]_{ss,bulk}$ values for both reactor depths (9.6×10^{-14} and 8.2×10^{-14} M for 5 and 20 cm depths, respectively). The exogenous mechanism was less important for sunlight inactivation of PV3,[6] which was reflected by relatively small PV3 k_2 measured in the wetland water, the dominance of k^{L}_{endo}, and the decrease in PV3 k^{L}_{obs} and k^{L}_{tot} with increased water column depth due to light attenuation.

Measured and Modeled Inactivation Rates in the Open-Water Wetland. F+RNA coliphages were used as indicator viruses to monitor inactivation within the open-water cell. Monitoring data were pooled for each month (Figure 2)

DOI: 10.1021/es5049754
Environ. Sci. Technol. XXXX, XXX, XXX−XXX

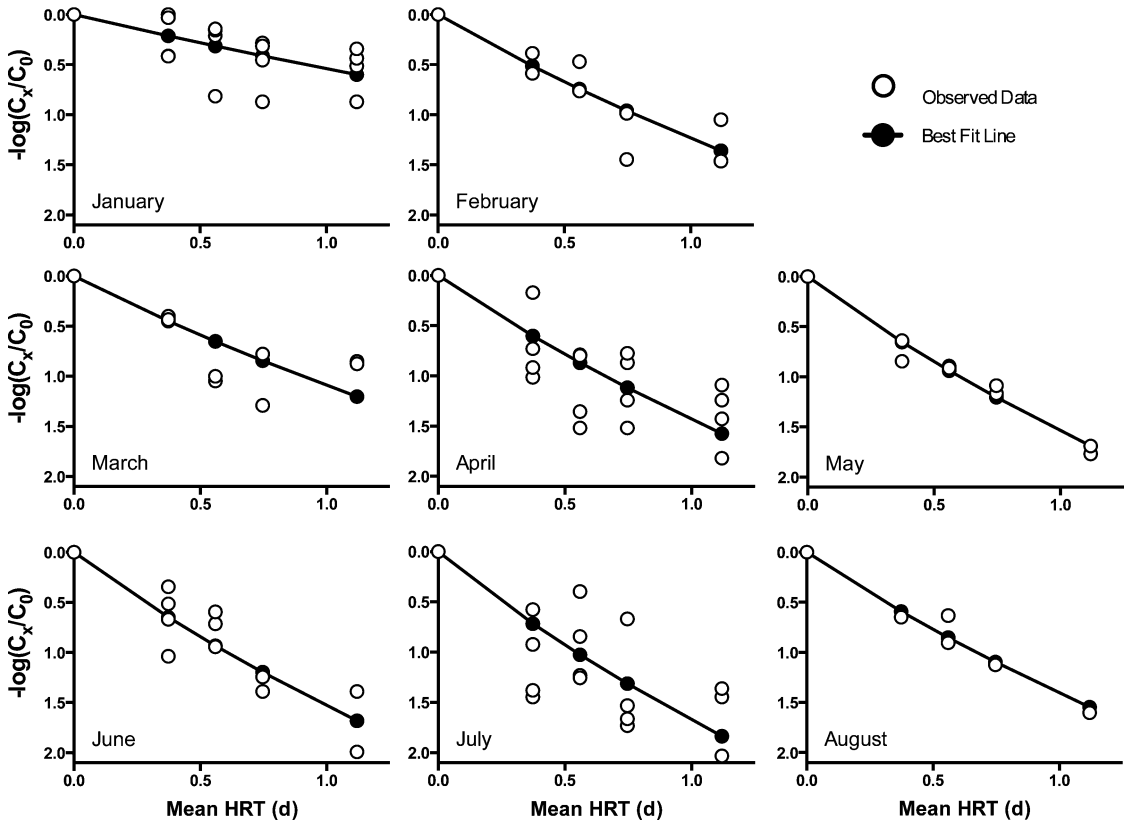

Figure 2. F+RNA coliphage monitoring data from the Discovery Bay wastewater treatment wetland open-water cell. Best fit lines were plotted using the Wehner−Wilhelm equation and the best fit k_{obs}^{W} for each month. Somatic coliphage data are presented in Figure S3 of the Supporting Information.

and used to calculate monthly best fit k_{obs}^{W} values (Table S4, Supporting Information, and used to construct curves in Figure 2; somatic coliphage data are presented in Figure S3, Supporting Information).

We compared predicted MS2 k_{tot}^{W} values with F+RNA coliphage k_{obs}^{W} values measured in the open-water cell. Although we also modeled PV3 inactivation rates in the open-water cell, we were unable to compare modeled rates with observed inactivation rates because PV3 was not expected to be available in the wetland for monitoring. Furthermore, a suitable indicator virus for PV3 is currently unknown. MS2 k_{endo}^{W} values predicted by the PAS modeling approach were, on average, 65% lower than those predicted by the tUVB approach (Figure S11, Supporting Information). However, due to the dominance of the exogenous mechanism for MS2, this translated to only a 10% difference between k_{tot}^{W} predicted with k_{endo}^{W} from the two approaches. Given that the PAS model accounts for the effect of individual UVB wavelengths, we focus on MS2 k_{tot}^{W} predicted with the PAS model for the remainder of this analysis. Modeled MS2 k_{tot}^{W} values were in reasonable agreement with measured F+RNA coliphage k_{obs}^{W} values (Figure 3), although predicted inactivation rates were between 11% (June) and 50% (February) lower than the measured values (Table S4, Supporting Information). Therefore, modeled values provided conservative estimates of F+RNA coliphage inactivation. A breakdown of the predicted contribution of the endogenous and exogenous mechanisms to MS2 and PV3 k_{tot}^{W} is presented in Figure S12 (Supporting Information). The exogenous mechanism was predicted to dominate MS2 inactivation, while the endogenous mechanisms were predicted to dominate PV3 inactivation.

The model was able to predict the annual pattern in inactivation rates caused by seasonal changes in sunlight intensity, length of day, and solar zenith angle. However, we did not study the effect of cloud cover on inactivation rates, and samples were only collected after periods of full sunlight exposure. Additionally, we did not include the effect of evaporation in the modeling equations. Jasper et al.[25] calculated that evaporation had only a minor influence on k_{obs} for chemical photolysis in the open-water cell, even during summer when evaporation is expected to be highest.

There are a few hypotheses regarding the underprediction of k_{obs}^{W}. First, MS2 may not be a perfect indicator for all type of F+RNA coliphages. Love et al.,[10] for example, found that F+RNA isolates collected from a southern California beach had average endogenous sunlight inactivation rates that were 2 times faster than that of MS2 (n = 4). Furthermore, it is unknown if the susceptibility of MS2 to exogenous inactivation compares well to that of all other F+RNA coliphages.

A simple sensitivity analysis (described in the Supporting Information) found that the model was most sensitive to changes in $E_d(0,\lambda)$, $[^1O_2]_{ss,bulk}$, and k_2 (Figure S2, Supporting Information). $^1O_2$ concentrations and $E_d(0,\lambda)$ input to the wetland model were predicted values and may not be accurate. The assumptions used to correct inactivation rates for mixing within, and shading by, the biomat may also not accurately resemble conditions in the wetland. When inactivation rates were predicted over a 20 cm, well-mixed water column without correction for the biomat, we found MS2 k_{tot}^{W} to be more similar

DOI: 10.1021/es5049754
Environ. Sci. Technol. XXXX, XXX, XXX−XXX

to F+RNA coliphage k^{W}_{obs} (Figure S13, Supporting Information). Additional possibilities for the underprediction of k^{W}_{obs} include the occurrence of removal mechanisms that were not captured by the model (e.g., predation and other dark processes), changes in water quality through the cell, and hydraulic properties that may have differed from our assumptions (e.g., mixing, d, and total HRT). The total HRT, for example, may have been greater than 1.12 d, given that we did not achieve 100% recovery during the tracer test; also, the inlet flow rate likely varied between sampling days. A greater HRT would result in a lower F+RNA coliphage k^{W}_{obs} calculated by the Wehner−Wilhelm equation (Figure S1, Supporting Information).

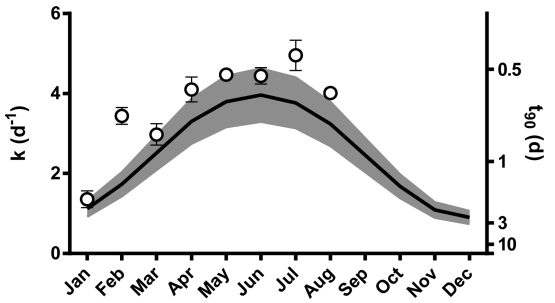

Figure 3. Measured F+ coliphage k^{W}_{obs} values (white dots) and modeled MS2 k^{W}_{tot} values (black line; PAS model) in the Discovery Bay wastewater treatment wetland open-water cell. The secondary y-axis is the time (d) for 90% virus inactivation. Error bars on k^{W}_{obs} are root-mean-square errors; the gray band around k^{W}_{tot} is the calculated standard error.

MS2 k_2. On average, k_2 for MS2 and $^1O_2$ in water from the Discovery Bay open-water cell was found to be 3.3 times larger than k_2 calculated for other environmental waters in previous studies (Figure S14, Supporting Information).[6,11] The k_2 calculated in Discovery Bay wetland water was also greater than k_2 reported for MS2 and $^1O_2$ using Rose Bengal as the sensitizer (e.g., 1.4×10^{12} M^{-1} h^{-1} by Kohn and Nelson[11] and 1.3×10^{12} M^{-1} h^{-1} by Mattle et al.[14]). Several factors—including the involvement of reactive species other than $^1O_2$ and interaction between viruses and photosensitizers—could contribute to this difference.

$OH^{\bullet}$ and ^3OM have been found to contribute to MS2 inactivation.[9,14] Nitrate in the wetland water (average concentration in influent was 20.7 mg/L-N)[35] led to $[OH^{\bullet}]_{ss,bulk}$ that ranged between approximately 0.5×10^{-15} M (pH 10) and 3×10^{-15} M (pH 7).[24] While $OH^{\bullet}$ may lead to increased inactivation of MS2, Mattle et al.[14] estimated that $^1O_2$ was responsible for 72% of the exogenous inactivation of MS2 in water from a waste stabilization pond, with ^3OM contributing 18% and $OH^{\bullet}$ contributing only 7%. Thus, it is unlikely that inactivation by these reactive species was sufficient to account for the high apparent k_2 value. Nonetheless, ongoing research in our group indicates a rather complicated relationship between reactive triplet states and MS2 inactivation. Assuming that the reactivity of a given excited triplet state toward a target virus can vary depending on the molecular structure and thus the chemical properties of its ground state, it is possible that triplet states generated in the wetland water were more effective at inactivating MS2 than photosensitizers present in other waters that have been studied.

Due to their reactivity and short lifetime, reactive species concentrations are greater close to their source of production than in bulk solution.[31] Therefore, for any reactive species involved in MS2 inactivation, virus−photosensitizer interaction (resulting from water matrix conditions or photosensitizer properties that promote association) results in greater virus exposure to oxidants and therefore a greater apparent k_2.[6,12] For example, the relatively high divalent cation concentration measured in the Discovery Bay wetland water (between 1.4 and 1.5 mM Mg^{2+}) may have increased virus−photosensitizer association, and therefore the apparent k_2, through cation bridging between negatively charged viruses and NOM.[12,36]

The properties of organic matter in the Discovery Bay wetland, and potentially wastewater-derived organic matter in general [e.g., effluent organic matter (EfOM)], may also lead to a greater k_2. For example, EfOM tends to consist of smaller molecules than terrestrially derived NOM.[37,38] The MS2 capsid contains 32 pores that allow access to the virus interior,[39] and MS2 RNA has been found to be an important target of oxidative damage.[40] A hypothesis is that if smaller sized EfOM has better access to MS2 pores and RNA (which also depends on EFOM and water quality characteristics), this photosensitizer could cause a greater apparent k_2. More research is needed on the effect of EfOM characteristics on k_2. A related research question is whether biomat-derived compounds in the water column contribute to exogenous inactivation.

The MS2 inactivation rate model is very sensitive to k_2, given the importance of the exogenous mechanism to this virus. Unfortunately, however, k_2 must be determined through laboratory experiments and is therefore the most resource intensive input to measure. Further research is needed to determine the factors that govern the apparent k_2, so that k_2 can be predicted for photosensitizers in other water bodies and for other viruses. Additionally, knowledge of the factors contributing to k_2 could allow for the design of unit-process wetlands that enhance exogenous inactivation by placing wetland cells that produce more virucidal photosensitizers upstream of open-water cells.

Challenges with the Total UVB Model. In laboratory experiments, the tUVB model predicted k^{L}_{endo} values in PBS within 10% of measured inactivation rates for both MS2 and PV3. However, given that shorter wavelength light is more damaging to viruses than longer wavelength light,[21,41] there is an inherent bias in the tUVB model, which weighs damage from all UVB wavelengths equally. Different solar simulators—or sunlight at different latitudes, elevations, or seasons—can have different ratios of short to long wavelength UVB irradiance. If, for example, two light sources have the same total UVB irradiance, but one has more short wavelength irradiance, these two sources will cause different rates of inactivation, which would result in different β values (i.e., due to the same total UVB irradiance but different k_{obs} values). This challenge was exemplified in experiments conducted by Nguyen et al.,[22] during which MS2 k_{obs} values in sensitizer-free water were measured for 1 h intervals with exposure to natural sunlight. When comparing hourly k_{obs} values with the sum of UVB irradiance during that hour, β was 0.04 m^2 W^{-1} h^{-1} (Figure S15, Supporting Information), which is one-third of the magnitude of β used in the present study to predict MS2 $k_{endo,tUVB}$.

Another context in which the tUVB model is expected to introduce error is in modeling inactivation at depth. In natural waters, short wavelength light is absorbed more strongly than

DOI: 10.1021/es5049754
Environ. Sci. Technol. XXXX, XXX, XXX−XXX

longer wavelength light (Figure S5, Supporting Information). As a result, the ratio of short to long wavelength UVB irradiance decreases with the depth of the water column, and β values determined using irradiance measured at the water surface would not be valid at greater depths. As an example, in the present study, the ratio of $\sum_{280}^{300}\langle E_0(z,\lambda)\rangle$ to $\sum_{300}^{320}\langle E_0(z,\lambda)\rangle$ was 0.093 for incident light and an average of 0.080 and 0.067 for well-mixed depths of 5 and 20 cm. This effect would result in an overprediction of k_{endo} in deeper well-mixed water columns when using the tUVB model.

Mattle et al.[14] developed a more fundamental approach to predict endogenous inactivation rates: determining virus-specific quantum yields. However, this approach also gives equal weight to photons of different wavelengths and to date has only been tested using a single simulated light source. Although the PAS model has the advantage of weighting the damage caused by different wavelengths, Nguyen et al.[22] discuss several shortcomings that still need to be addressed.

Using the Model To Design Treatment Wetlands. Additional work is needed to more comprehensively assess the variability of the model inputs and the sensitivity of the model to a range of field conditions (e.g., see the paper by Liu et al.[42]). Nonetheless, the current inactivation rate model can be used to provide insight into wetland design. For open-water wetlands, Jasper and Sedlak[24] developed an approach to estimate the wetland surface area required for 90% removal of a given trace organic contaminant that depends on wetland depth and flow rate and the contaminant's removal rate, constant (e.g., k_{tot}). To apply this approach to virus inactivation, we determined the surface areas needed to treat 1 million gallons of wastewater per day (MGD = 3.79×10^3 m^3/d) to achieve 1-, 2- and 3-log inactivation of MS2 in a system similar to the Discovery Bay open-water cell (i.e., PAS k_{endo} model; [DOC] = 8 mg/L-C, z = 20 cm, biomat thickness of 5 cm, sunlight irradiance predicted at 40° N latitude; see the Supporting Information for calculations). The surface area needed for 2-log inactivation of MS2 was predicted to range from 4 ha MGD^{-1} (HRT = 1.6 d) in June to 17 ha MGD^{-1} (HRT = 6.7 d) in December (Figure 4); these areas are similar to those of constructed wetlands currently used in the United States.[24]

A second way to use the model is to optimize the surface area to depth ratio of open-water cells; such an analysis is useful for determining the costs and benefits of constructing a deeper wetland versus purchasing more land to provide a greater surface area. We calculated the surface areas required per MGD to achieve 2-log removal of MS2 and PV3 in well-mixed water depths that range from 20 cm to 1 m with exposure to sunlight in June and December (Figure 4); 1 m depth is typical of traditional maturation ponds.[43] The required surface area decreased with increasing depth for both viruses due to longer HRT. However, for depths greater than 50 cm, little gain in reducing the surface area was predicted. However, a critical outstanding question is whether the mixing dynamics or ecology of the open-water cell would change with increased depth; if the water column becomes stratified or dominated by planktonic organisms (i.e., as in maturation ponds), it could reduce the inactivation rates.

The land area required for 2-log inactivation of MS2 was predicted to be greater than that of PV3 in June; however, the opposite was true in December due to lower light intensity and a low PV3 k_{endo}. These results indicate that MS2 serves as a conservative indicator for PV3 inactivation in June but not in December. By extension, F+RNA coliphages may not be a conservative process indicator for human virus inactivation in surface waters under some conditions.

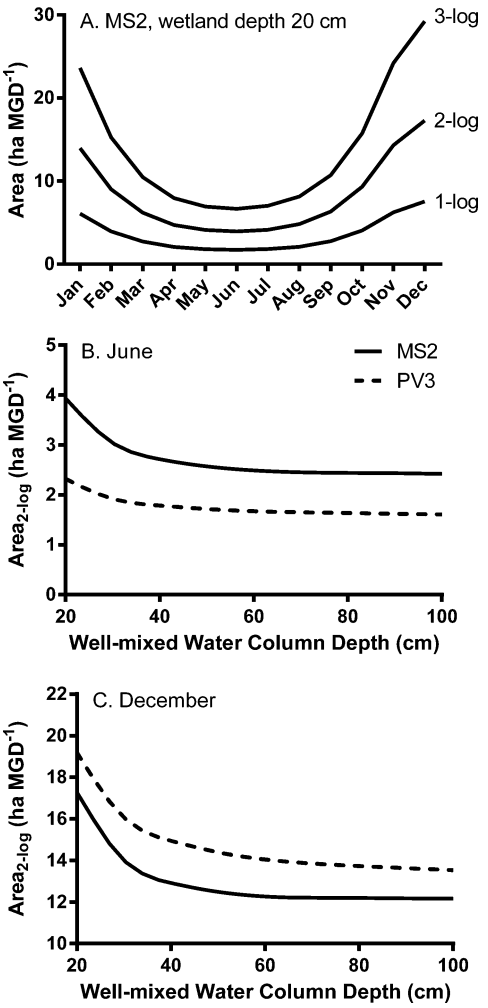

Figure 4. (A) Open-water wetland surface areas required to treat 1 million gallons of wastewater per day (MGD) to the specified MS2 treatment objectives (i.e., 1-, 2-, or 3-log inactivation), given a well-mixed water column depth of 20 cm. (B,C) Surface areas required per MGD to achieve 2-log inactivation of MS2 and PV3 for a range of well-mixed water column depths in June and December. The sunlight spectra used to model k_{tot}^{W} were for 40° N latitude. Uncertainty values around calculated areas are presented in Figure S17 of the Supporting Information.

■ ASSOCIATED CONTENT

Supporting Information

Detailed methodology, results of sensitivity analyses, a summary of model terms and equations, supporting figures referenced in the text, and tables listing spectral sensitivity coefficients for the MS2 photoaction spectrum, inputs to SMARTS, and measured and modeled sunlight inactivation rates for all viruses are provided in the Supporting Information. This material is available free of charge via the Internet at http://pubs.acs.org.

■ AUTHOR INFORMATION

Corresponding Author

*Phone: 510-643-5023; e-mail: karanelson@berkeley.edu.

DOI: 10.1021/es5049754
Environ. Sci. Technol. XXXX, XXX, XXX−XXX

Present Address

[‖]J.W.: Department of Chemical Engineering and Water Innovation & Research Centre (WIRC), University of Bath, Claverton Down, Bath BA2 7AY, United Kingdom.

Notes

The authors declare no competing financial interest.

■ ACKNOWLEDGMENTS

This research was supported by the National Science Foundation (Grant CBET-0853568) and the Engineering Research Center for Re-inventing the Nations Urban Water Infrastructure (ReNUWIt; Grant EEC-1028968). J.W. was supported by a postdoctoral scholarship from the Swiss National Science Foundation (Grant PBEZP2-142887). We thank Ann Fisher of the University of California, Berkeley, tissue culture facility for cell culture assistance. We thank Justin Jasper and Samantha Beardsley for their assistance and discussions. We thank Virgil Koehne, manager of the Town of Discovery Bay, and Alex Horne for designing and managing the Discovery Bay treatment wetlands.

■ REFERENCES

(1) Shilton, A. N. *Pond Treatment Technology*; IWA Publishing: London, U.K., 2005.

(2) Kadlec, R. H.; Wallace, S. *Treatment Wetlands*; CRC Press: Boca Raton, FL, 2009.

(3) Jasper, J. T.; Nguyen, M. T.; Jones, Z. L.; Ismail, N. S.; Sedlak, D. L.; Sharp, J. O.; Luthy, R. G.; Horne, A. J.; Nelson, K. L. Unit process wetlands for removal of trace organic contaminants and pathogens from municipal wastewater effluents. *Environ. Eng. Sci.* **2013**, *30* (8), 421−436.

(4) Davies-Colley, R.; Donnison, A.; Speed, D.; Ross, C.; Nagels, J. Inactivation of faecal indicator microorganisms in waste stabilisation ponds: interactions of environmental factors with sunlight. *Water Res.* **1999**, *33* (5), 1220−1230.

(5) Davies-Colley, R. J.; Craggs, R. J.; Park, J.; Sukias, J. S. P.; Nagels, J. W.; Stott, R. Virus removal in a pilot-scale 'advanced' pond system as indicated by somatic and F-RNA bacteriophages. *Water Sci. Technol.* **2005**, *51* (12), 107−110.

(6) Silverman, A. I.; Peterson, B. M.; Boehm, A. B.; McNeill, K.; Nelson, K. L. Sunlight inactivation of human viruses and bacteriophages in coastal waters containing natural photosensitizers. *Environ. Sci. Technol.* **2013**, *47* (4), 1870−1878.

(7) Romero, O. C.; Straub, A. P.; Kohn, T.; Nguyen, T. H. Role of temperature and suwannee river natural organic matter on inactivation kinetics of rotavirus and bacteriophage MS2 by solar irradiation. *Environ. Sci. Technol.* **2011**, *45* (24), 10385−10393.

(8) Romero-Maraccini, O. C.; Sadik, N. J.; Rosado-Lausell, S. L.; Pugh, C. R.; Niu, X.-Z.; Croué, J.-P.; Nguyen, T. H. Sunlight-induced inactivation of human Wa and porcine OSU rotaviruses in the presence of exogenous photosensitizers. *Environ. Sci. Technol.* **2013**, *47* (19), 11004−11012.

(9) Rosado-Lausell, S. L.; Wang, H.; Gutierrez, L.; Romero-Maraccini, O. C.; Niu, X.-Z.; Gin, K. Y. H.; Croué, J.-P.; Nguyen, T. H. Roles of singlet oxygen and triplet excited state of dissolved organic matter formed by different organic matters in bacteriophage MS2 inactivation. *Water Res.* **2013**, *47* (14), 4869−4879.

(10) Love, D. C.; Silverman, A.; Nelson, K. L. Human virus and bacteriophage inactivation in clear water by simulated sunlight compared to bacteriophage inactivation at a southern California beach. *Environ. Sci. Technol.* **2010**, *44* (18), 6965−6970.11.

(11) Kohn, T.; Nelson, K. L. Sunlight-mediated inactivation of MS2 coliphage via exogenous singlet oxygen produced by sensitizers in natural waters. *Environ. Sci. Technol.* **2007**, *41* (1), 192−19712.

(12) Kohn, T.; Grandbois, M.; McNeill, K.; Nelson, K. L. Association with natural organic matter enhances the sunlight-mediated inactivation of MS2 coliphage by singlet oxygen. *Environ. Sci. Technol.* **2007**, *41* (13), 4626−4632.

(13) Bosshard, F.; Armand, F.; Hamelin, R.; Kohn, T. Mechanisms of human adenovirus inactivation by sunlight and UVC light as examined by quantitative PCR and quantitative proteomics. *Appl. Environ. Microbiol.* **2013**, *79* (4), 1325−1332.

(14) Mattle, M. J.; Vione, D.; Kohn, T. Conceptual model and experimental framework to determine the contributions of direct and indirect photoreactions to the solar disinfection of MS2, phiX174, and adenovirus. *Environ. Sci. Technol.* **2015**, *49* (1), 334−342.

(15) White, G. C. *Handbook of Chlorination and Alternative Disinfectants*; John Wiley & Sons, Inc.: Hoboken, NJ, 1999.

(16) Langlais, B.; Rechhow, D. A.; Brink, D. R. *Ozone in Water Treatment, Applications and Engineering*; Lewis Publishers, Inc.: Fort Worth, TX, 1991.

(17) Hijnen, W. A. M.; Beerendonk, E. F.; Medema, G. J. Inactivation credit of radiation for viruses, bacteria and protozoan (oo)cysts in water: a review. *Water Res.* **2006**, *40* (1), 3−22.

(18) Sinton, L. W.; Hall, C. H.; Lynch, P. A.; Davies-Colley, R. J. Sunlight inactivation of fecal indicator bacteria and bacteriophages from waste stabilization pond effluent in fresh and saline waters. *Appl. Environ. Microbiol.* **2002**, *68* (3), 1122−1131.

(19) Sinton, L. W.; Finlay, R. K.; Lynch, P. A. Sunlight inactivation of fecal bacteriophages and bacteria in sewage-polluted seawater. *Appl. Environ. Microbiol.* **1999**, *65* (8), 3605−3613.

(20) Verbyla, M. E.; Mihelcic, J. R. A review of virus removal in wastewater treatment pond systems. *Water Res.* **2014**, *71*, 107−124.

(21) Fisher, M. B.; Love, D. C.; Schuech, R.; Nelson, K. L. Simulated sunlight action spectra for inactivation of MS2 and PRD1 bacteriophages in clear water. *Environ. Sci. Technol.* **2011**, *45* (21), 9249−9255.

(22) Nguyen, M. T.; Silverman, A. I.; Nelson, K. L. Sunlight inactivation of MS2 coliphage in the absence of photosensitizers: modeling the endogenous inactivation rate using a photoaction spectrum. *Environ. Sci. Technol.* **2014**, *48* (7), 3891−3898.

(23) Sigstam, T.; Gannon, G.; Cascella, M.; Pecson, B. M.; Wigginton, K. R.; Kohn, T. Subtle differences in virus composition affect disinfection kinetics and mechanisms. *Appl. Environ. Microbiol.* **2013**, *79* (11), 3455−3467.

(24) Jasper, J. T.; Sedlak, D. L. Phototransformation of wastewater-derived trace organic contaminants in open-water unit process treatment wetlands. *Environ. Sci. Technol.* **2013**, *47* (19), 10781−10790.

(25) Jasper, J. T.; Jones, Z. L.; Sharp, J. O.; Sedlak, D. L. Biotransformation of trace organic contaminants in open-water unit process treatment wetlands. *Environ. Sci. Technol.* **2014**, *47* (19), 10781−10790.

(26) Nguyen, M. T.; Jasper, J. T.; Boehm, A. B.; Nelson, K. L. Sunlight inactivation of fecal indicator bacteria in open-water unit process treatment wetlands: modeling endogenous and exogenous inactivation rates. Manuscript in preparation.

(27) Kirk, J. T. O. *Light and Photosynthesis in Aquatic Ecosystems*; Cambridge University Press: Cambridge, U.K., 2010.

(28) Bodrato, M.; Vione, D. APEX (aqueous photochemistry of environmentally occurring xenobiotics): a free software tool to predict the kinetics of photochemical processes in surface waters. *Environ. Sci.: Processes Impacts* **2014**, *16*, 732−740.

(29) Zepp, R. G.; Cline, D. M. Rates of direct photolysis in aquatic environment. *Environ. Sci. Technol.* **1977**, *11* (4), 359−366.

(30) Gueymard, C. A. Interdisciplinary applications of a versatile spectral solar irradiance model: a review. *Energy* **2005**, *30* (9), 1551−1576.

(31) Latch, D. E.; McNeill, K. Microheterogeneity of singlet oxygen distributions in irradiated humic acid solutions. *Science* **2006**, *311*, 1743−1747.

(32) Haag, W. R.; Hoigne, J. Singlet oxygen in surface waters. 3. Photochemical formation and steady-state concentrations in various types of waters. *Environ. Sci. Technol.* **1986**, *20* (4), 341−348.

DOI: 10.1021/es5049754
Environ. Sci. Technol. XXXX, XXX, XXX−XXX

(33) Haag, W. R.; Hoigné, J.; Gassman, E.; Braun, A. Singlet oxygen in surface waters—Part I: furfuryl alcohol as a trapping agent. *Chemosphere* **1984**, *13* (5−6), 631−640.
(34) Wehner, J. F.; Wilhelm, R. H. Boundary conditions of flow reactor. *Chem. Eng. Sci.* **1956**, *6* (2), 89−93.
(35) Jasper, J. T.; Jones, Z. L.; Sharp, J. O.; Sedlak, D. L. Nitrate removal in shallow, open-water treatment wetlands. *Environ. Sci. Technol.* **2014**, *48* (19), 11512−11520.
(36) Gerba, C. P. Applied and theoretical aspects of virus adsorption to surfaces. *Adv. Appl. Microbiol.* **1984**, *30*, 133−168.
(37) Quaranta, M. L.; Mendes, M. D.; MacKay, A. A. Similarities in effluent organic matter characteristics from Connecticut wastewater treatment plants. *Water Res.* **2012**, *46* (2), 284−294.
(38) Cabaniss, S. E.; Zhou, Q.; Maurice, P. A.; Chin, Y.-P.; Aiken, G. R. A log-normal distribution model for the molecular weight of aquatic fulvic acids. *Environ. Sci. Technol.* **2000**, *34* (6), 1103−1109.
(39) Hooker, J. M.; Kovacs, E. W.; Francis, M. B. Interior surface modification of bacteriophage MS2. *J. Am. Chem. Soc.* **2004**, *126* (12), 3718−3719.
(40) Wigginton, K. R.; Pecson, B. M.; Sigstam, T.; Bosshard, F.; Kohn, T. Virus inactivation mechanisms: impact of disinfectants on virus function and structural integrity. *Environ. Sci. Technol.* **2012**, *46* (21), 12069−12078.
(41) Lytle, C. D.; Sagripanti, J.-L. Predicted inactivation of viruses of relevance to biodefense by solar radiation. *J. Virol.* **2005**, *79* (22), 14244−14252.
(42) Liu, L.; Fu, X.; Wang, G. Parametric study of fate and transport model of *E. coli* in the nearshore region of southern Lake Michigan. *J. Environ. Eng.* **2014**, *140* (9), A5013001.
(43) Mara, D. D. Pond process design—a practical guide. In *Pond Treatment Technology*; Shilton, A. N., Ed.; IWA Publishing: London, U.K., 2005.

DOI: 10.1021/es5049754
Environ. Sci. Technol. XXXX, XXX, XXX−XXX